

## **Highly-Flexible, Low-Cost, All Stainless Steel Mesh-based Dye-Sensitized Solar Cells**

Heng Li,<sup>a</sup> Qing Zhao,<sup>\*a</sup> Hui Dong,<sup>b</sup> Qianli Ma,<sup>a</sup> Wei Wang,<sup>a</sup> Dongsheng Xu,<sup>b</sup> and

Dapeng Yu<sup>\*a</sup>

<sup>a</sup> State Key Laboratory for Mesoscopic Physics, School of Physics, Peking University, Beijing 100871, P. R. China.

<sup>b</sup> State Key Laboratory for Structural Chemistry of Unstable and Stable Species, College of Chemistry and Molecular Engineering, Peking University, Beijing 100871, P. R. China

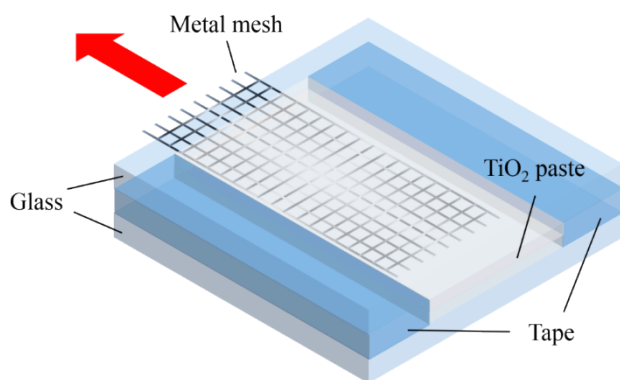


**Fig. S1** Schematic illustration of the drawing press technique for the first step TiO<sub>2</sub> layer deposition.

**Drawing press:** Put the mesh on the glass between two pieces of tape (thickness: 60  $\mu\text{m}$ ). Apply a portion of paste near the middle of mesh. Cover the mesh and tape with another glass. Press the upper glass to spread the paste in the gap between the two glass pieces. Draw the mesh out from the gap slowly.

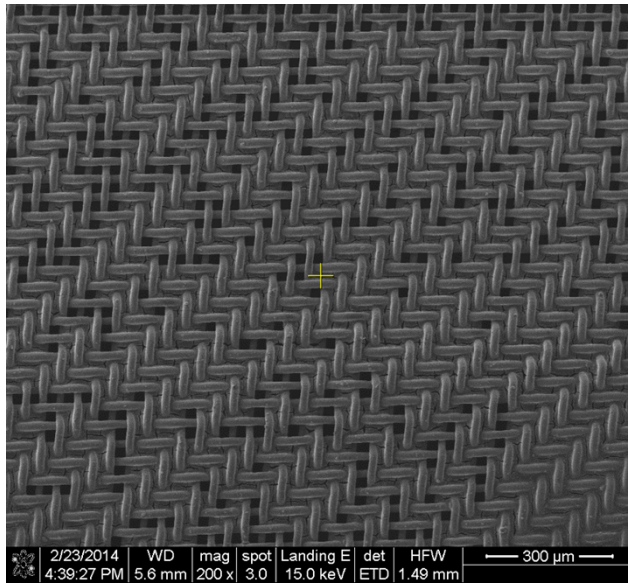


**Fig. S2** SEM image of the stainless steel mesh only after  $\text{TiO}_2$  paste deposition by doctor blading without using the two-step deposition method. Many voids between mesh wires can not be covered by  $\text{TiO}_2$  layer.

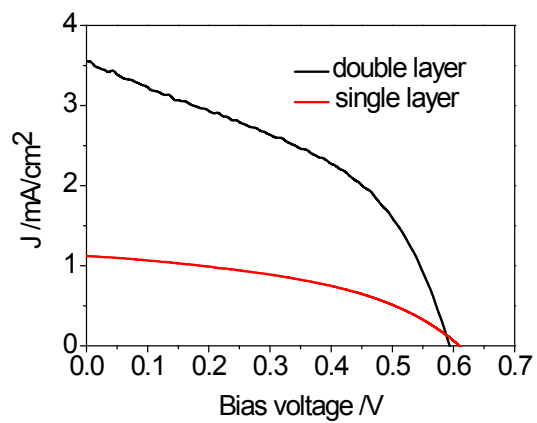


**Fig. S3**  $J$ - $V$  curves of DME-DSSCs before and after the second step  $\text{TiO}_2$  layer deposition.

## **Analyses for asymmetric design of photoanode**

The photon absorption layer on the upper side is neither too thin to absorb most incident light nor too thick to reduce recombination current and series resistance. The supporting layer after first step deposition on the underside is neither too thin to sustain the photo absorption layer nor too thick to ensure efficient ion transmission in electrolyte. The supporting layer would never be illuminated, but it is located between the photo absorption layer and counter electrode. Thus, the electrolyte has higher  $I_3^-$  concentration above and higher  $I^-$  concentration below. The diffusion of the ions is affected by the supporting layer which has mesoporous nanostructure. Additionally, the supporting layer would oxidize the  $I^-$  anions, and it can be regarded as a parallel cell in dark, which reduces the open voltage and fill factor of the entire solar cell. The electrochemical impedance of the solar cell will increase with the thickness of the supporting layer. So the first supporting layer should be as thin as possible. Note this negative impact brought by the  $TiO_2$  layer where the sun never shines has not been considered in previous work.

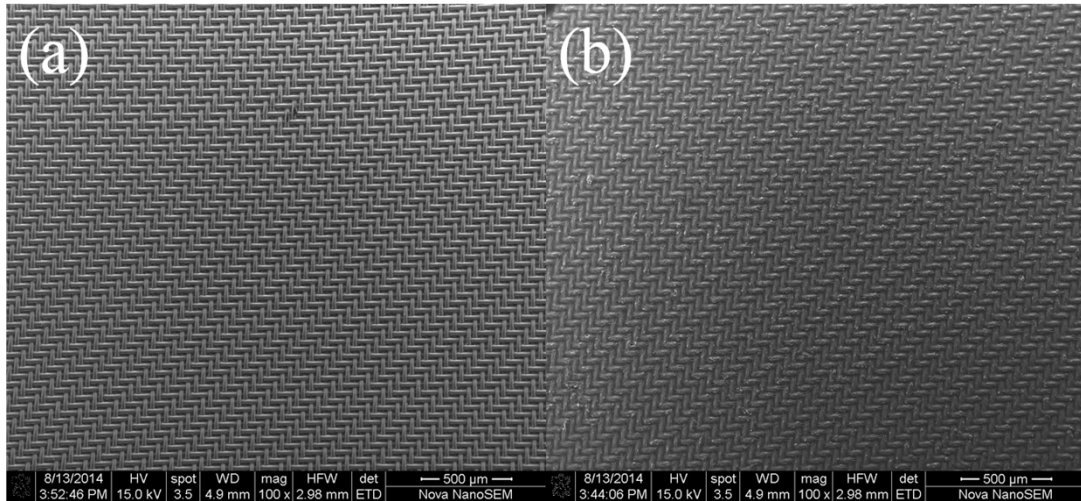


**Fig. S4** (a) SEM image the anode's back side, facing the counter electrode, equivalent to the mesh after the first step  $\text{TiO}_2$  coating. (b) SEM image of the anode's front side, facing light source directly. They demonstrate that the  $\text{TiO}_2$  coating is very uniform in large-scale.

### Bending test

The bending tests were controlled by hand. The bending radius ( $R$ ) were determined by the length of the device ( $L$ ) and the distance between the edges of the device ( $W$ ) as shown in Fig. S5. One bending cycle took about 1-2 seconds.

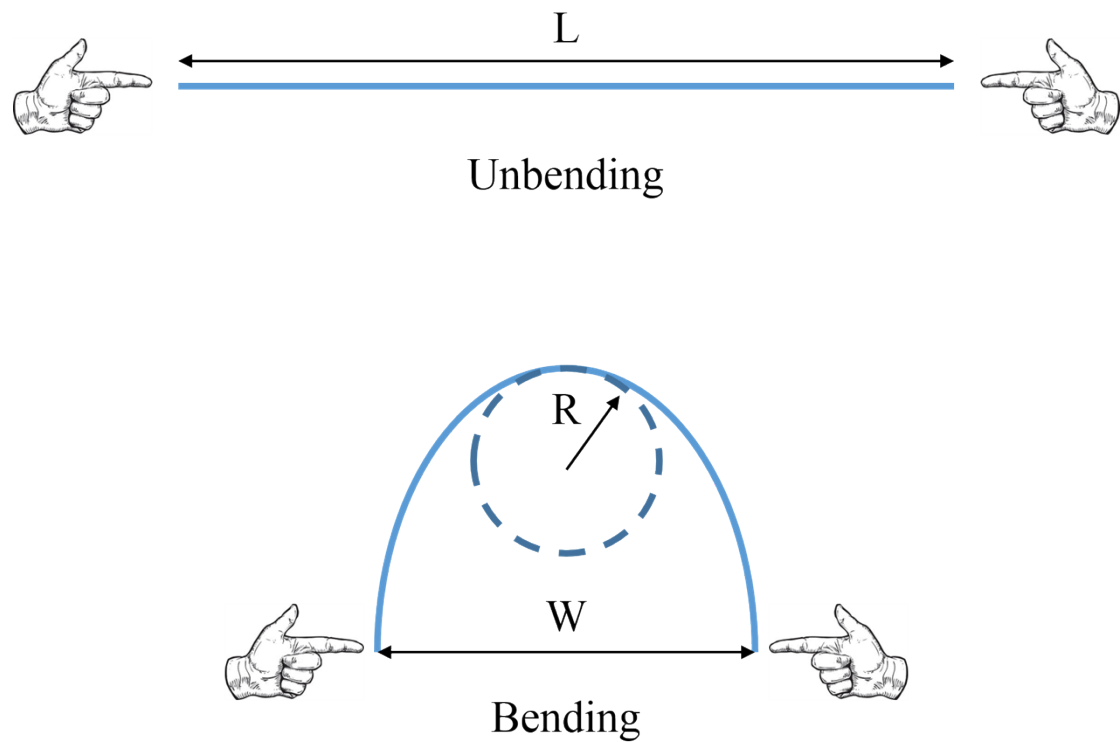


**Fig. S5** The schematic illustration of the bending test by hand. The blue solid line represents the device.

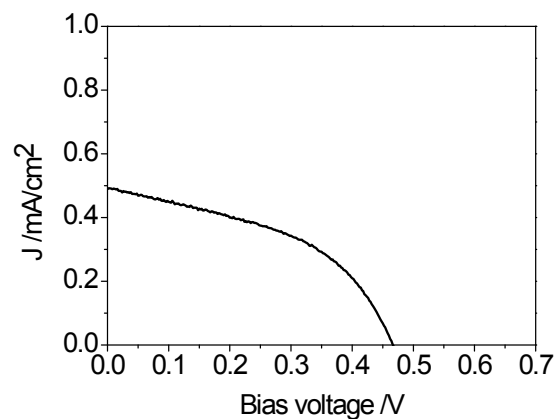


**Fig. S6** *J-V* curve of DSSC using TiO<sub>2</sub> coated stainless steel foil as photoanode. It shows much worse performance compared to mesh based DSSCs.

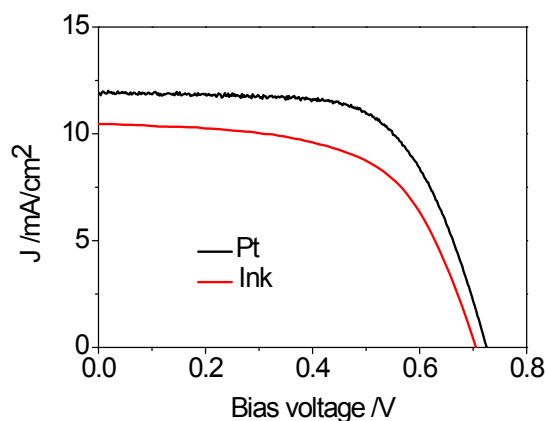


**Fig. S7**  $J$ - $V$  curves of conventional DSSCs using Pt coated FTO glass and carbon ink coated FTO glass as counter electrode for comparison.

In order to further demonstrate the function of commercial ink as effective counter electrode material in DSSCs, platinum coated FTO glass and ink (carbon nanoparticles) coated FTO glass were compared as counter electrode in conventional sandwich type DSSCs. The thickness of carbon nanoparticle layer can be controlled by repeating dip-coating (2  $\mu\text{m}$  each time). Fig. S5 showed the  $J$ - $V$  characteristics of the DSSCs with platinum counter electrode (10 nm) and with ink counter electrode (2  $\mu\text{m}$ ). The  $J_{sc}$  and FF of the latter are a little less than but comparable to those of the former, which indicates that commercial ink can act as an effective counter electrode material in DSSCs. The observed difference of the two DSSCs is on account of the catalytic activity of cathode materials. The use of commercial carbon ink as counter electrode of DSSCs can significantly decrease the fabrication cost of DSSCs.

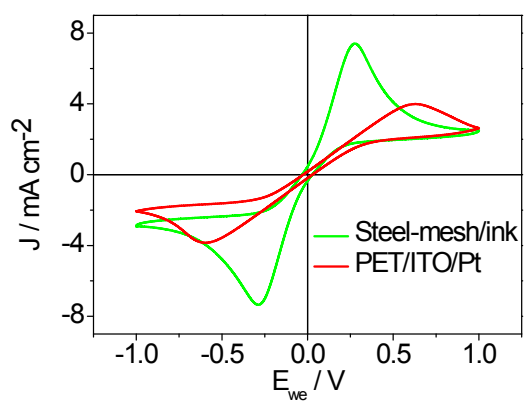


**Fig. S8** Cyclic voltammograms ( $0.1 \text{ V s}^{-1}$ ) of carbon ink coated stainless steel mesh and Pt coated PET/ITO film.

	$V_{oc} / V$	$J_{sc} / mA\ cm^{-2}$	FF / %	PCE / %
<b>Type A</b>	0.60	3.54	43	0.92
<b>Type B</b>	0.60	3.83	40	0.93
<b>Type C</b>	0.58	2.66	38	0.59
<b>Type D</b>	0.57	2.81	39	0.63

**Table S1.** The table of photovoltaic performance according to different devices, from Type A to D.